Brief Communication | Genitourinary Imaging

http://dx.doi.org/10.3348/kjr.2015.16.4.846
pISSN 1229-6929 · eISSN 2005-8330
Korean J Radiol 2015;16(4):846-852

Korean Journal of Radiology
KJR

Multiparametric Magnetic Resonance Imaging Characteristics of Prostate Tuberculosis

Yue Cheng, MD, Lixiang Huang, MD, Xiaodong Zhang, MD, Qian Ji, MD, PhD, Wen Shen, MD, PhD

All authors: Department of Radiology, Tianjin First Central Hospital, Tianjin 300192, China

Objective: To describe the multiparametric magnetic resonance imaging (MRI) appearance of prostate tuberculosis.
Materials and Methods: Six patients with prostate tuberculosis were analyzed retrospectively. The mean age of the patients was 60.5 years (range, 48–67 years). The mean prostate specific antigen concentration was 6.62 ng/mL (range, 0.54–14.57 ng/mL). All patients underwent a multiparametric MRI examination.
Results: The histopathological results were obtained from biopsies in four men and from transurethral resection of the prostate in two men after the MRI examination. Nodular (33%, 2/6 patients) and diffuse lesions (67%, 4/6 patients) were seen on MRI. The nodular lesions were featured by extremely low signal intensity (similar to that of muscle) on T2-weighted imaging (T2WI). The T2WI signal intensity of the diffuse lesions was low but higher than that of muscle, which showed high signal intensity on diffusion weighted imaging and low signal intensity on an apparent diffusion coefficient map. MR spectroscopic imaging of this type showed a normal-like spectrum. Abscesses were found in one patient with the nodular type and in one with the diffuse type.
Conclusion: The appearance of prostate tuberculosis on MRI can be separated into multiple nodular and diffuse types. Multiparametric MRI may offer useful information for diagnosing prostate tuberculosis.
Index terms: *Prostate tuberculosis; MRI; Multiple nodular; Diffuse*

INTRODUCTION

Tuberculosis usually involves the upper urinary tract, particularly the kidney (1). However, prostate tuberculosis is relatively rare; thus, the magnetic resonance imaging (MRI) appearances of prostate tuberculosis has been reported sporadically (1-4). The purpose of this study was to assess the MRI findings of prostate tuberculosis. Knowledge of the MRI appearance of prostate tuberculosis will facilitate the differential diagnosis.

Received January 22, 2015; accepted after revision April 21, 2015.
Corresponding author: Wen Shen, MD, PhD, Department of Radiology, Tianjin First Central Hospital, No.24 Fu Kang Road, Nan Kai District, Tianjin 300192, China.
• Tel: (8622) 23626501 • Fax: (8622) 23361365
• E-mail: shenwen66happy@163.com

MATERIALS AND METHODS

This retrospective study was approved by the local ethics committee of Tianjin First Central Hospital, and informed consent was waived. We identified six cases of prostate tuberculosis confirmed by histopathological examination at our hospital from January 2008 to September 2013. The mean age of the patients was 60.5 years (range, 48–67 years). Their clinical symptoms were dysuria and increased frequency and urgency of urination. One case had fever (37.8°C). A digital rectal examination (DRE) indicated an enlarged prostate with hard texture but no tenderness or nodularity. The mean prostate specific antigen (PSA) concentration was 6.62 ng/mL (range, 0.54–14.57 ng/mL). Chest radiography revealed old tuberculosis in one patient. No evidence of other active foci of respiratory or urogenital

Korean Journal of Radiology
KJR

tuberculosis was detected in any of the cases. None of the patients underwent Bacillus Calmette-Guerin (BCG) therapy for bladder cancer. All patients underwent prostate MRI, including T1-weighted imaging (T1WI), T2-weighted imaging (T2WI), and diffusion weighted imaging (DWI). An apparent diffusion coefficient (ADC) map was generated from the DWI data. Under the suspicion of prostate cancer, one patient also underwent additional MR spectroscopic imaging (MRS). A histological diagnosis was rendered with tissue obtained from transrectal ultrasound (TRUS)-guided biopsy in four men and with tissue obtained at the time of a transurethral resection of the prostate in two men. Eight systematic cores were taken from all patients during the TRUS-guided biopsy. All the biopsies were performed after the MRI examination, and the interval between MRI and biopsy was 3–15 days (mean, 7 days). One of the patients who received a biopsy also underwent epididymectomy, and abscesses were found during the surgery. Prostate tuberculosis was diagnosed based on the presence of Langhans cells, caseous necrosis, and acid-fast bacilli (AFB). The histological analysis did not show evidence of prostate cancer in any of the patients.

MRI Protocol

The MRI examination was performed with a 3.0-T imaging unit (Magnetom Trio, Siemens Healthcare, Erlangen, Germany) with a pelvic phased-array surface coil. The following images were obtained: axial, coronal, and sagittal T2-weighted turbo spin-echo (SE) images (time of repetition [TR]/time of echo [TE], 4000/101 msec, 3 mm thickness); axial T1-weighted turbo SE images (TR/TE, 630/11 msec; 3 mm thickness); axial free-breathing DWI (b values, 0 and 1000 sec/mm^2; 3 mm thickness); three-dimensional MRS data were acquired using a point resolved spectroscopic sequence (TR/TE, 650/120 msec; acquisition time, 10 minutes). The MRS data were post-processed with the spectroscopic software that accompanied the MRI scanner. Choline, creatine, and citrate metabolites were quantified through prior knowledge of metabolite peak locations and widths. The integral ratio was used for further analysis, i.e., choline plus creatine/citrate area (CC/C).

Imaging Analysis

All imaging studies were reviewed retrospectively by consensus of two radiologists with 5 and 8 years experience. The MRI features of prostate tuberculosis were separated into diffuse and nodular types, which showed a diffuse decrease in T2 signal intensity without a clear margin or well-defined focal T2 hypointense area, respectively. According to Suzuki et al. (2), the signal and range of diffuse lesions, as well as the size, number, and signal of nodular lesions were evaluated. In addition, whether the lesion extended into the transition zone (TZ) or periprostatic tissue was also evaluated.

RESULTS

Pathological Findings

All positive cores showed typical features of granulomatous prostatitis with epithelioid cells, multinucleated giant cells, and lymphocyte infiltration (Fig. 1A). Central caseous necrosis foci were seen in some cores. AFB staining was positive in three cases (Fig. 1B).

MRI Appearance

The main MRI findings are summarized in Table 1.

The nodular type was found in two of six (33%) patients. MRI showed multiple nodules in the peripheral zone (PZ) and the TZ. Seven nodules were found in the PZ and 10 were found in the TZ. Nodule diameter was 4–18 mm. All nodular lesions showed were isointense on T1WI, extremely low signal intensity (similar to that of muscle) on T2WI (Figs. 2A, B, 3A), and low signal intensity on DWI and the ADC map (Fig. 2C, D). None of the nodules protruded into the periprostatic tissue. A hyperintense area was seen in one of the nodules from patient no. 1 on T2WI (Fig. 3B) and showed markedly high signal intensity on DWI (Fig. 3C, D). This patient also presented with an enlarged right seminal vesicle and right epididymis, as well as multiple lymph nodes in the right groin with similar abnormal signal intensity. Abscesses of the epididymis were confirmed during the epididymectomy.

Diffuse lesions were found in four (67%) of six patients. Only the PZ was involved in three patients; two and one diffuse lesions were seen in bilateral and unilateral PZs, respectively. Both the PZ and TZ were involved in the fourth patient. All diffuse lesions showed isointense signal on T1WI and low signal intensity on T2WI (but higher than that of muscle) (Fig. 4A). Restricted diffusion was identified on DWI. No diffuse lesion extended into the periprostatic tissue. Multiple nodules were detected in the TZ of patient no. 4, which showed markedly high and low signal intensities on DWI and the ADC map, respectively (Fig. 4B, C). This patient also underwent a MRS examination,

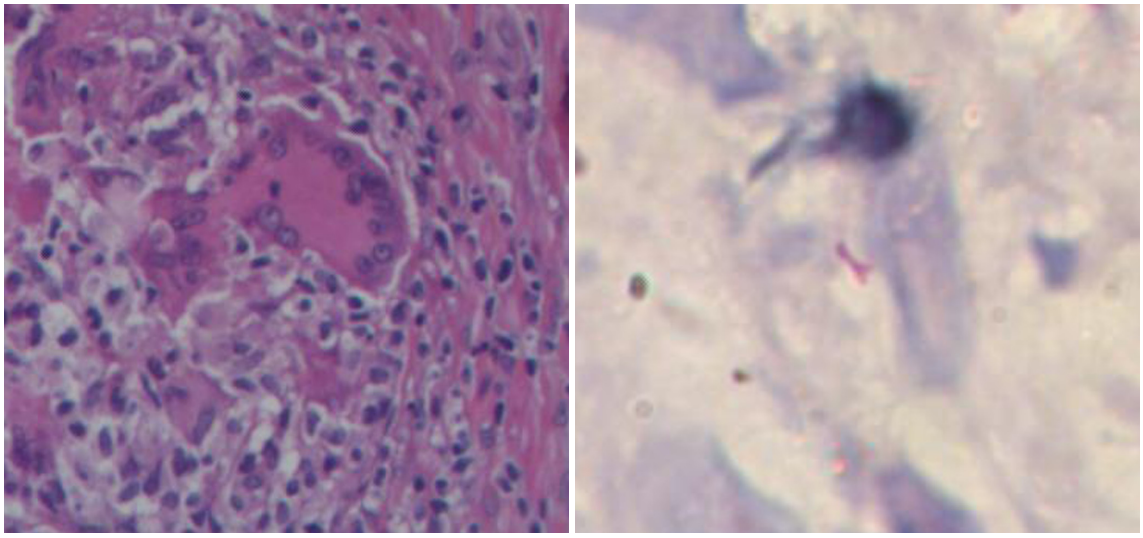

A B

Fig. 1. Pathological specimens obtained at biopsy.
A. Hematoxylin and eosin staining reveals presence of multinucleated giant cells (x 400). **B.** Acid-fast staining shows bacilli (x 400).

Table 1. MR Findings of Patients with Prostate Tuberculosis

Case	Age	Type	Localization		SI				MRS	Abscess
			TZ	PZ	T1WI	T2WI	DWI	ADC Map		
1	48	Nodular	+	+/bilateral	Iso	Extremely low	Low	Low		+
2	63	Nodular	+	+/bilateral	Iso	Extremely low	Low	Low		-
3	64	Diffuse	-	+/unilateral (R)	Iso	Low	Slightly high	Slightly low		-
4	67	Diffuse	+	+/bilateral	Iso	Low	High	Low	Normal	+
5	62	Diffuse	-	+/bilateral	Iso	Low	Slightly high	Slightly low		-
6	59	Diffuse	-	+/bilateral	Iso	Low	High	Low		-

Plus (+) means presence and minus (–) means absence of lesions. ADC = apparent diffusion coefficient, DWI = diffusion-weighted imaging, MRS = MR spectroscopic imaging, PZ = peripheral zone, SI = signal intensity, T1WI = T1-weighted imaging, T2WI = T2-weighted imaging, TZ = transition zone

the CC/C ratios from the hypointense areas were within the normal range (< 0.86) (Fig. 4D).

The MRI appearances of two cases (one nodular type and one diffuse type, patient nos. 1 and 4) showed characteristic findings of abscesses, particularly a markedly high signal on DWI and a low signal on the ADC map.

DISCUSSION

Genitourinary tuberculosis accounts for 5–10% of extrapulmonary cases in developed countries and 15–20% of cases in developing countries (5). Nevertheless, isolated prostate tuberculosis is uncommon, particularly in immunocompetent patients, and most cases are detected incidentally. Diagnosing prostate tuberculosis is challenging, as the symptoms are nonspecific, including dysuria with increased frequency and urgency, except when it involves the epididymis (6). A DRE often reveals an enlarged prostate with or without pain, hard areas, and the results cannot be differentiated from prostate hyperplasia and cancers (7). Urinalysis and a urine culture are usually negative. PSA may be normal or increased. A positive tuberculin skin test may suggest a tuberculosis infection but cannot be relied on and a negative test does not preclude the diagnosis. A prostate biopsy and demonstration of AFB is the mainstay for the diagnosis (8).

Because of its relative rarity, the MRI characteristics of prostate tuberculosis have not been described extensively and only a few cases have been reported. One case of prostate tuberculosis showed a diffuse radiating streaky low signal intensity lesion on T2WI (watermelon skin sign), and this sign was considered specific for prostate tuberculosis (9). No watermelon signs were observed in our cases or in the report of Chen et al. (1). Bour et al. (4) reported three cases of prostate tuberculosis after BCG therapy. The lesions showed hypo-intense signals on T2WI, restricted

Korean Journal of Radiology
KJR

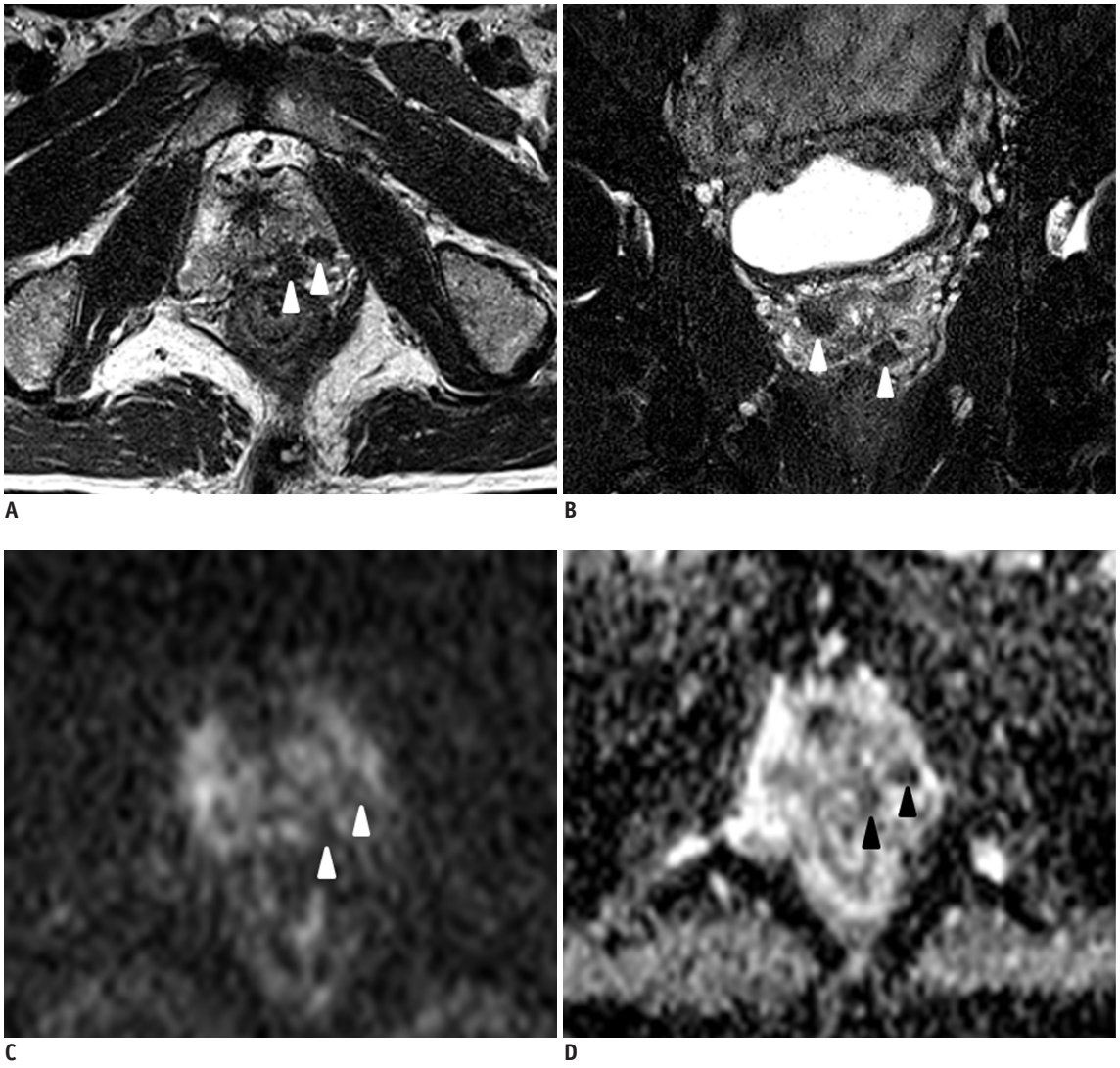

Fig. 2. Nodular type of prostate tuberculosis in 63-year-old man.
A. Axial T2-weighted image (T2WI) shows multiple extremely low signal intensity nodules in left peripheral zone (arrowheads). **B.** Coronal T2WI shows multiple nodules in peripheral and transition zones. Images **C** and **D** were taken from same slice as image **A**. Nodules were hypointense on diffusion-weighted image **(C)** and apparent diffusion coefficient map **(D)**.

diffusion on DWI, and moderate enhancement on dynamic contrast-enhanced MRI (DCE-MRI). The MRI appearances of our cases were separated into diffuse and nodular types, in agreement with the study of Suzuki et al. (2) and Ma et al. (3). Nodular type is characterized by markedly low signal intensity on T2WI, which is significant for the differential diagnosis from prostate cancer. Paramagnetic substances in tuberculomas, such as macrophage-laden oxygen-free radicals, were thought to be the factor that reduces the T2 values (10). The markedly low signal intense nodules on T2WI should be differentiated from calcification, which can be confirmed on a computed tomography scan.

The diffuse lesions showed lower signal intensity than the normal PZ on T2WI, but not as low as that of a nodular lesion. The diffuse lesions showed high signal intensity on DWI and low signal intensity on the ADC map. These findings reflect inflammatory cell infiltration in these lesions. These findings mimic those found in patients with diffuse prostate carcinoma. Some MRS characteristics for distinguishing prostate tuberculosis from cancer have been reported (1). The CC/C ratio is elevated in cancer tissue, which is caused by a diminished capacity of malignant epithelial cells to synthesize and secrete citrate and higher levels of choline-containing compounds. Prostate cancer should be considered when the CC/C ratio in the PZ is > 0.86 (11). Prostate tuberculosis is a benign disease and does not cause remarkably accelerated cell proliferation or eliminate citrate metabolism; thus, the citrate level should

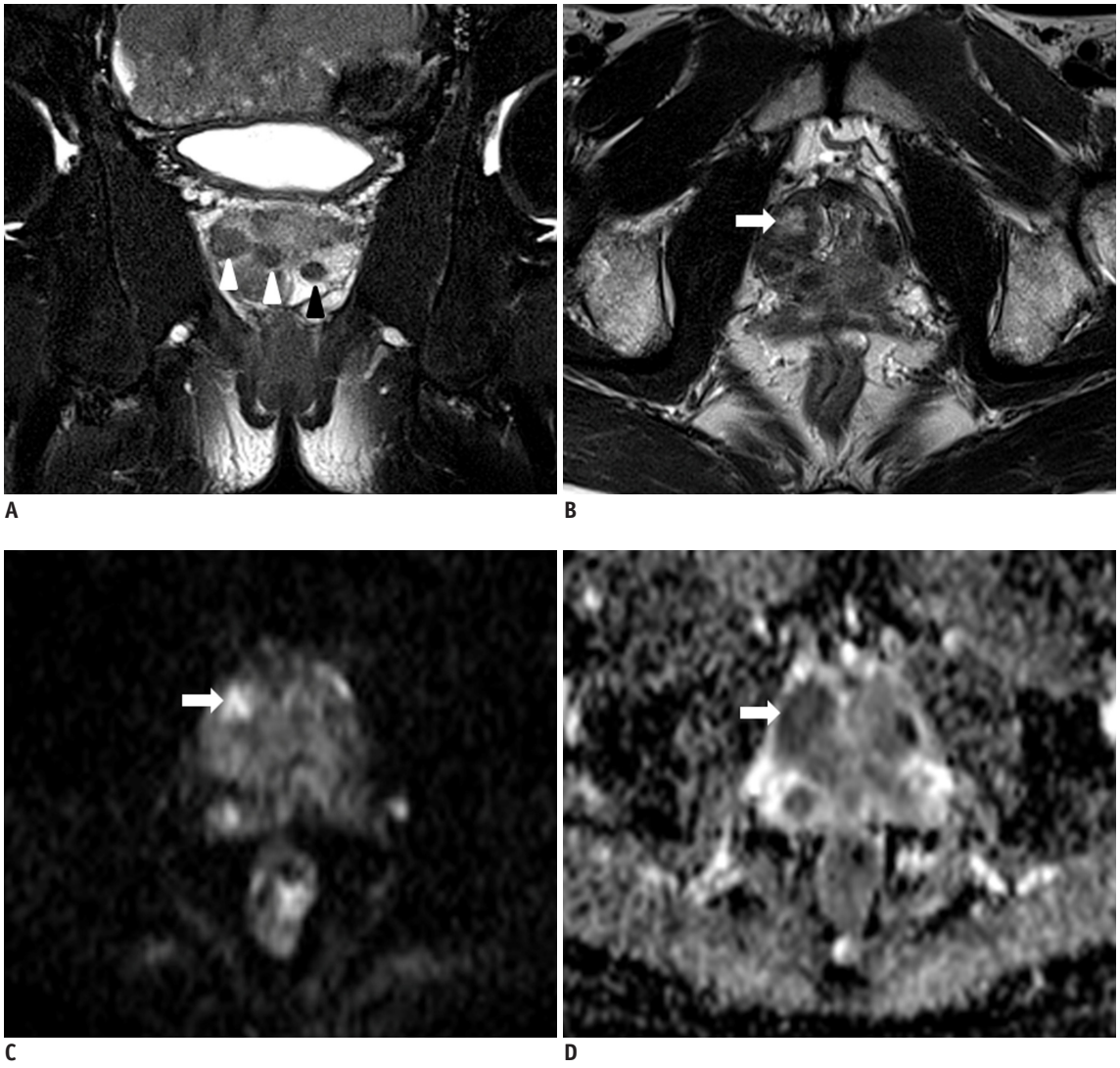

Fig. 3. Nodular type prostate tuberculosis in 48-year-old man.
(A) Coronal T2-weighted image (T2WI) shows multiple low signal intensity nodules (arrowheads) in prostate. Hyperintense area (arrow) was detected in nodule on T2WI **(B)**, which appeared as markedly high signal intensity on diffusion-weighted image **(C)** and relative low signal intensity on apparent diffusion coefficient map **(D)**.

be within the normal range. In our cases, all CC/C ratios from abnormal signal areas on T2WI were < 0.86, consistent with a previous report (1).

An abscess is rarely reported rare in patients with prostate tuberculosis, particularly in immunocompetent patients. Some cases of tubercular abscesses following intravesical BCG therapy have been reported (4, 12-14). In the present study, MRI showed necrotic areas in two cases that demonstrated characteristic features of a soft-organ abscess, i.e., hyperintense lesion on T2WI with markedly high signal intensity on DWI and markedly low signal intensity on the ADC map (15). Our cases suggest that occult tubercular abscesses are not rare. MRI is useful for evaluating the prevalence of occult caseous abscesses and for follow-up of patients after anti-tubercular treatment (4).

Our study had several limitations. First, the number of cases was small; thus, further studies are needed to confirm the characteristic MRI findings of prostate tuberculosis. Second, none of our patients underwent a DCE-MRI examination, which is important to distinguish between prostate tuberculosis and prostate cancer or to confirm an abscess.

In conclusion, nodular and diffuse prostate tuberculosis types were identified in this study. Although a definite diagnosis must be made after bacteriologic and microscopic examinations, multiparametric MRI may be helpful in the diagnosis.

Korean Journal of Radiology
KJR

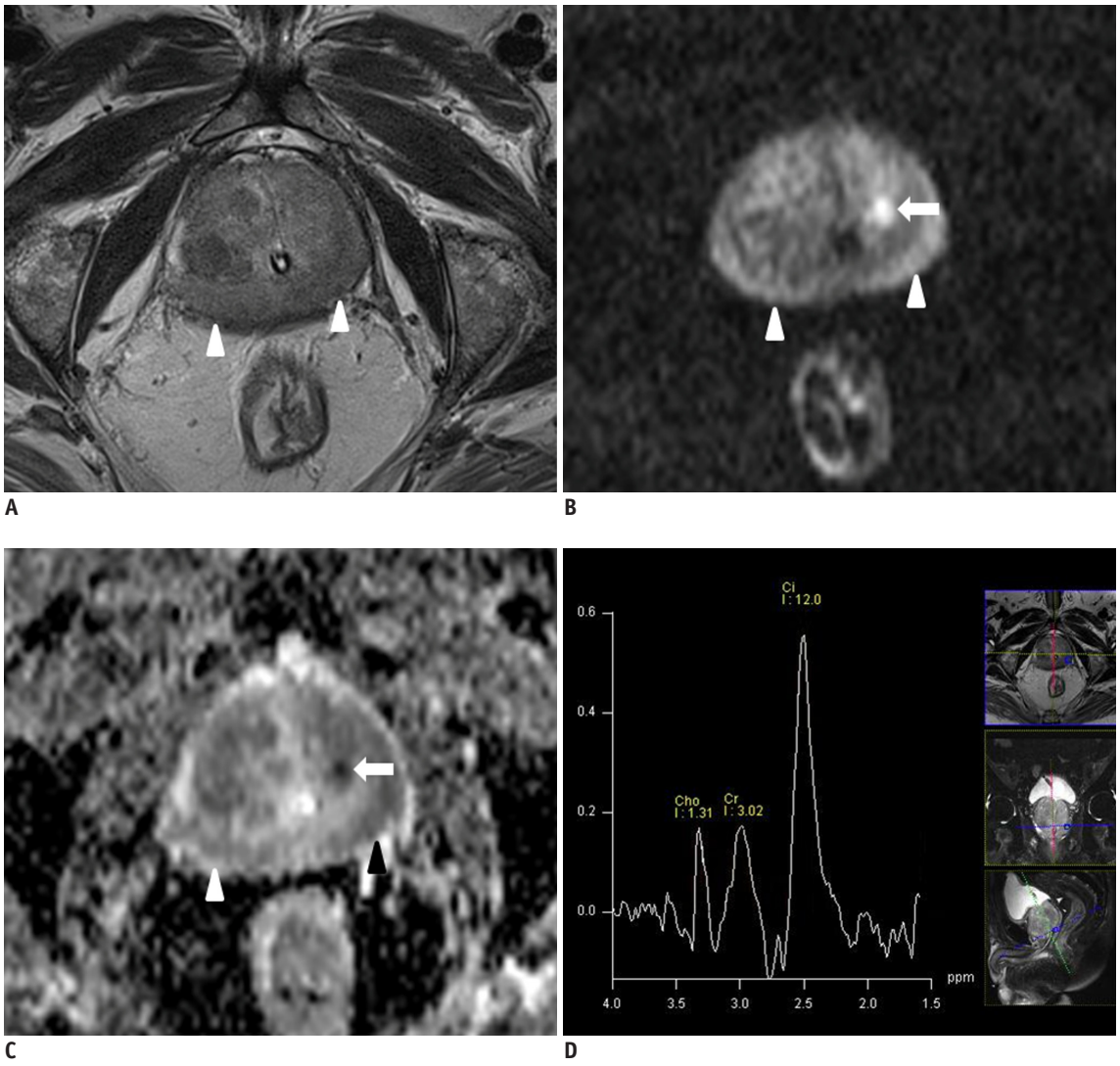

Fig. 4. Diffuse type prostate tuberculosis in 67-year-old man.
(A) Bilateral peripheral zone shows diffuse hypointensity (arrowheads) on T2-weighted image, high signal intently on diffusion weighted image (DWI), **(B)** low signal intensity on apparent diffusion coefficient (ADC) map **(C)** (arrowheads), and small patchy area (arrow) with markedly high signal intensity on DWI and markedly low signal intensity on ADC. **(D)** Magnetic resonance spectroscopic imaging of left peripheral zone reveals high peak of citrate and low peak of choline.

Acknowledgments

We acknowledge Dr. Pan-Li Zuo from Siemens Ltd. China for her help in optimizing the MR scan parameters.

REFERENCES

1. Chen Y, Liu M, Guo Y. Proton magnetic resonance spectroscopy in prostate tuberculosis. *Urology* 2010;75:1065-1066
2. Suzuki T, Takeuchi M, Naiki T, Kawai N, Kohri K, Hara M, et al. MRI findings of granulomatous prostatitis developing after intravesical Bacillus Calmette-Guérin therapy. *Clin Radiol* 2013;68:595-599
3. Ma W, Kang SK, Hricak H, Gerst SR, Zhang J. Imaging appearance of granulomatous disease after intravesical Bacille Calmette-Guerin (BCG) treatment of bladder carcinoma. *AJR Am J Roentgenol* 2009;192:1494-1500
4. Bour L, Schull A, Delongchamps NB, Beuvon F, Muradyan N, Legmann P, et al. Multiparametric MRI features of granulomatous prostatitis and tubercular prostate abscess. *Diagn Interv Imaging* 2013;94:84-90
5. Sáenz-Abad D, Letona-Carbajo S, Benito-Arévalo JL, Sanioaquín-Conde I, Ruiz-Ruiz FJ. Prostatic tuberculosis: case report. *Sao Paulo Med J* 2008;126:227-228
6. Kostakopoulos A, Economou G, Picramenos D, Macrichoritis C, Tekerlekis P, Kalliakmanis N. Tuberculosis of the prostate. *Int Urol Nephrol* 1998;30:153-157
7. López Barón E, Gómez-Arbeláez D, Díaz-Pérez JA. [Primary prostatic tuberculosis. Case report and bibliographic review]. *Arch Esp Urol* 2009;62:309-313
8. Ludwig M, Velcovsky HG, Weidner W. Tuberculous epididymo-

orchitis and prostatitis: a case report. *Andrologia* 2008;40:81-83
9. Wang JH, Sheu MH, Lee RC. Tuberculosis of the prostate: MR appearance. *J Comput Assist Tomogr* 1997;21:639-640
10. Chung MH, Lee HG, Kwon SS, Park SH. MR imaging of solitary pulmonary lesion: emphasis on tuberculomas and comparison with tumors. *J Magn Reson Imaging* 2000;11:629-637
11. Kurhanewicz J, Vigneron DB, Hricak H, Narayan P, Carroll P, Nelson SJ. Three-dimensional H-1 MR spectroscopic imaging of the in situ human prostate with high (0.24-0.7-cm3) spatial resolution. *Radiology* 1996;198:795-805
12. Caulier P, Yombi JC, Dufaux M, Feyaerts A, Abi AA, Hainaut P. Prostate abscess following intravesical BCG therapy. *Acta Clin Belg* 2009;64:436-437
13. Aust TR, Massey JA. Tubercular prostatic abscess as a complication of intravesical bacillus Calmette-Guérin immunotherapy. *Int J Urol* 2005;12:920-921
14. Matlaga BR, Veys JA, Thacker CC, Assimos DG. Prostate abscess following intravesical bacillus Calmette-Guerin treatment. *J Urol* 2002;167:251
15. Oto A, Schmid-Tannwald C, Agrawal G, Kayhan A, Lakadamyali H, Orrin S, et al. Diffusion-weighted MR imaging of abdominopelvic abscesses. *Emerg Radiol* 2011;18:515-524